Bayesian inference of binary black holes with inspiral-merger-ringdown waveforms using two eccentric parameters

gr-qc : 2309.15528

Antoni Ramos-Buades, Alessandra Buonanno, Jonathan Gair

Dutch-Belgian GW Meeting
October 23, 2023

Nikhef NWO

MAX-PLANCK-GESELLSCHAFT

Gravitational-wave observations

- Third-observing (O3) run of the LIGO, Virgo and KAGRA (LVK) detectors: ~ **90 binary black holes** (BBHs), **2 binary neutron star** (BNS) and **2 neutron-star black-hole** (NSBH) binaries [Abbot+2021,Nitz+2021, Olsen+2021].

- Analysis performed with multipolar waveform models for **quasi-circular** precessing-spin BBHs.

- **Most detections consistent with quasi-circular binaries**.

- In **O4** and **future detectors**, more likely to detect **eccentric** binaries.

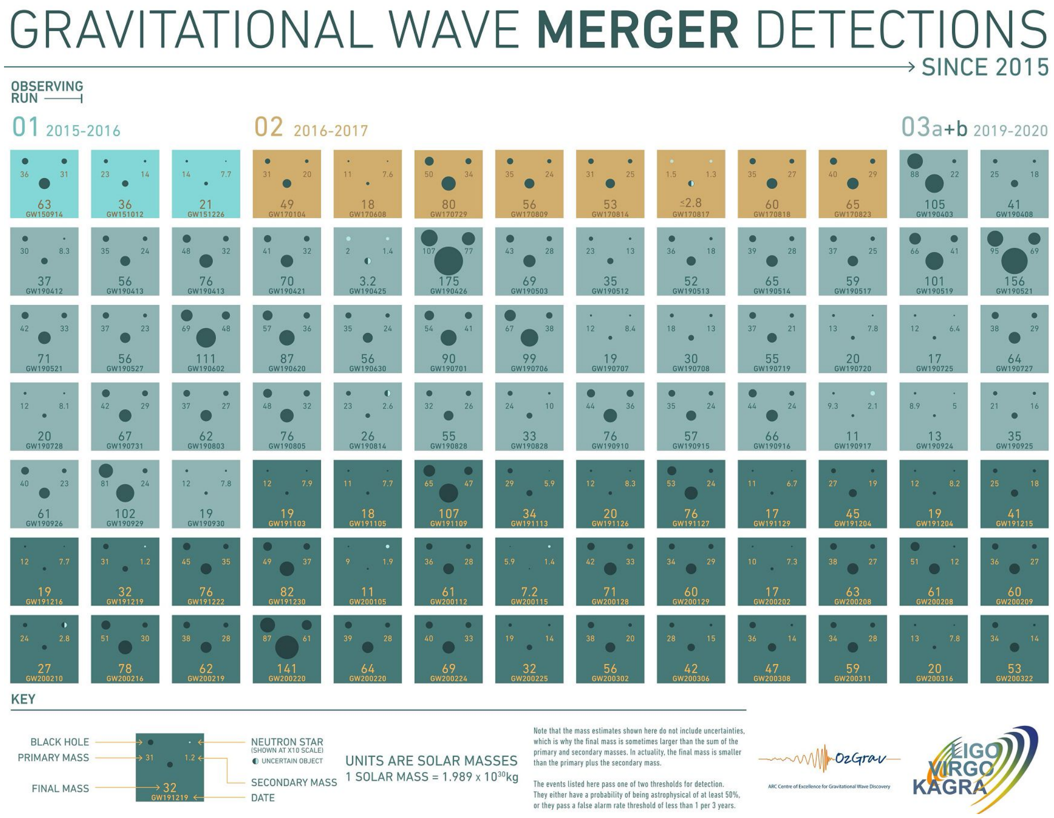

A waveform model for eccentric binary black holes

- Extension of accurate quasi-circular **multipolar aligned-spin SEOBNRv4HM** [Bohe+2017, Cotesta+2018] model to **eccentric** binaries (**SEOBNRv4EHM**) [Ramos-Buades+2021].

- It includes **eccentricity effects** to the **gravitational modes** (**22, 21, 33, 44, 55 modes**) up to **2PN order**, including spin-orbit and spin-spin effects [Khalil+2021].

- Two-parameter initial conditions : initial **eccentricity**, $0 < e_0 < 1$, and **relativistic anomaly**, $\zeta_0 \in [0, 2\pi]$, defined in the Keplerian parametrization:

$$r = \frac{p}{1 + e_0 \cos\zeta_0}, \quad p\text{: semi-latus rectum}$$

- Same **merger-ringdown** model as **SEOBNRv4HM** ⟶ system has **circularized** at **merger**.

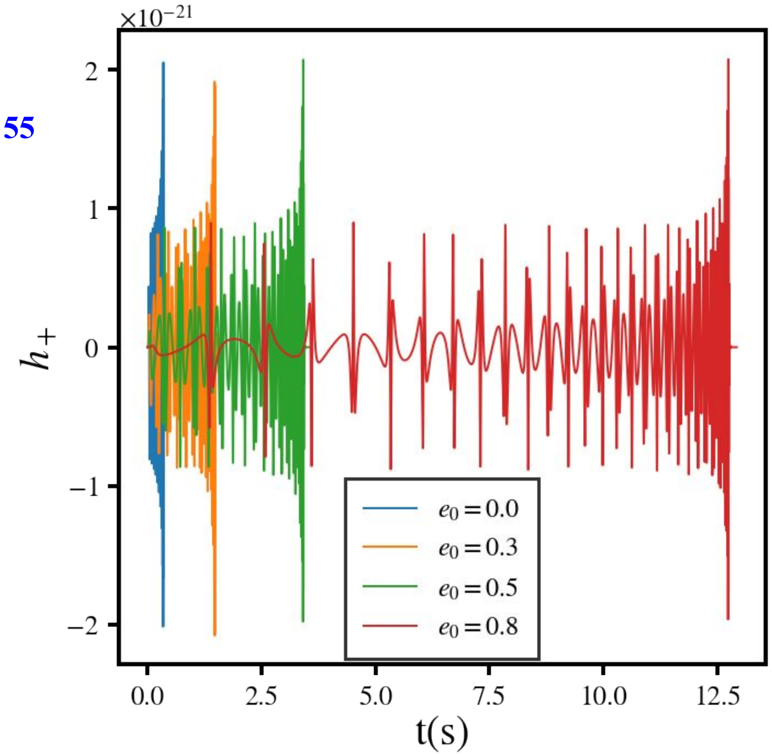

Initial conditions at an orbit-averaged frequency

- ICs at an **orbit-averaged orbital frequency**:
  - ~ constant merger time at fixed e_0.
  - Increase (decrease) of e_0 $\rightarrow$ decrease (increase) length evolution.

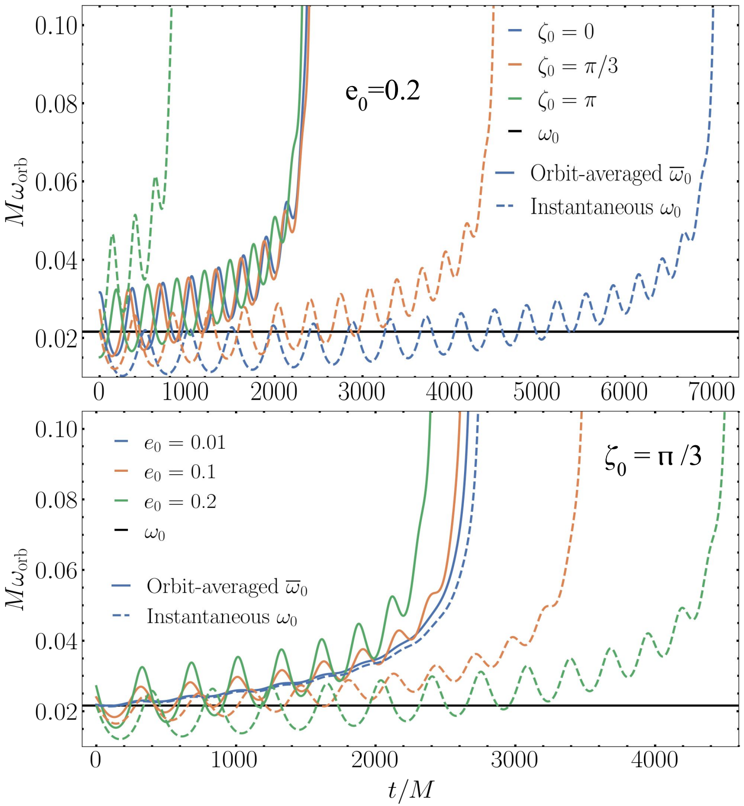

Test implications for parameter estimation computing **log-likelihood surfaces**.

New ICs **less structure** and **simpler** log-likelihood **surfaces**

$\Downarrow$

more efficient sampling of parameter space.

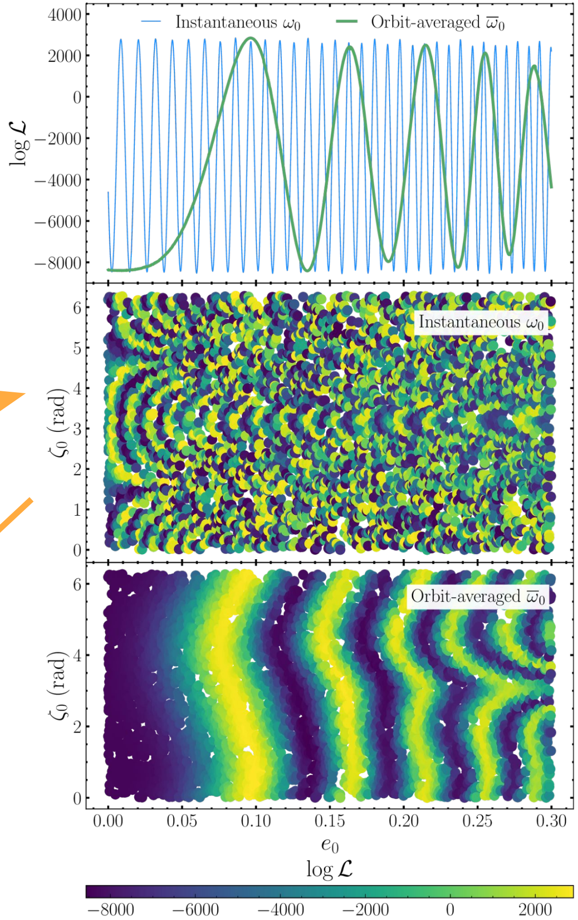

Numerical relativity injections

- Assess accuracy of **SEOBNRv4E_opt** with injections of **eccentric numerical relativity** (NR) **waveforms**.

- To compare NR and EOB eccentricities → common definition of **eccentricity based on the waveform** with correct Newtonian limit [Ramos-Buades+2022]:

$$e_{\rm gw} = \cos(\psi/3) - \sqrt{3}\sin(\psi/3),$$

$$\psi = \arctan\left(\frac{1-e_{\omega_{22}}^2}{2e_{\omega_{22}}}\right), e_{\omega_{22}} = \frac{\omega_{22,p}^{1/2} - \omega_{22,a}^{1/2}}{\omega_{22,p}^{1/2} + \omega_{22,a}^{1/2}}.$$

- **Mean anomaly** definition:

$$l_{\rm gw} = 2\pi\frac{t-t_i^p}{t_{i+1}^p - t_i^p}, \quad t_i^p\text{: i-th periastron passage.}$$

- Use highly efficient implementation in **gw_eccentricity** Python package [Shaikh+2023] on **samples at post-processing**.

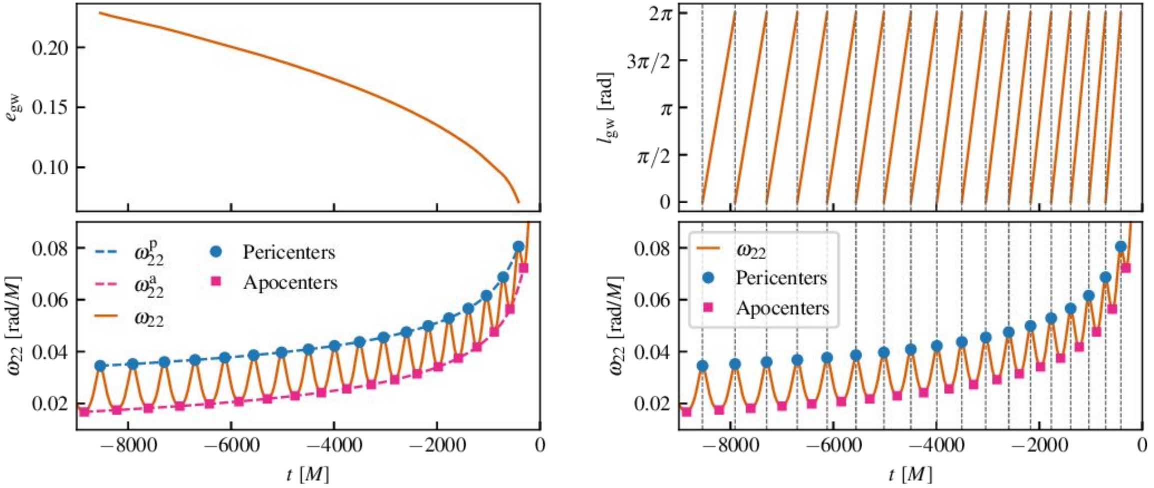

Figure from Shaikh+2023

Numerical relativity injections

- Inject 3 **equal-mass non-spinning** NR waveforms with e_0= (0.07,0.13,0.25) from the SXS catalog into zero noise:

$$q = 1, \quad \chi_{1,2} = 0, \quad M = 70 M_\odot, \quad \iota = 0, \quad \mathrm{SNR} = 20 \quad \text{at 20Hz}.$$

- NR waveforms with modes **l ≤ 8 modes**, and recover with **SEOBNRv4E_opt**.
- **Quasi-circular** parameters **accurately recovered** (bias in the d_L due to different mode content).
- **GW eccentricity** and **mean anomaly** are **accurately measured**.

Parameter	Injected value	SXS:1355	SXS:1359	SXS:1363
$M/M_\odot$	70.0	$70.87^{+2.47}_{-2.27}$	$70.41^{+2.45}_{-2.45}$	$69.81^{+2.32}_{-2.72}$
$\mathcal{M}/M_\odot$	30.47	$30.41^{+0.98}_{-0.95}$	$30.26^{+1.04}_{-1.14}$	$30.06^{+0.98}_{-1.21}$
$1/q$	1.0	$0.79^{+0.17}_{-0.19}$	$0.8^{+0.16}_{-0.19}$	$0.81^{+0.15}_{-0.17}$
$\chi_{\rm eff}$	0.0	$0.02^{+0.08}_{-0.08}$	$0.01^{+0.09}_{-0.1}$	$-0.0^{+0.08}_{-0.1}$
e_0	-	$0.06^{+0.05}_{-0.05}$	$0.14^{+0.03}_{-0.04}$	$0.29^{+0.09}_{-0.05}$
ζ_0	-	$2.23^{+1.37}_{-1.16}$	$1.01^{+4.67}_{-0.75}$	$3.28^{+1.6}_{-0.45}$
$\theta_{\rm JN}$	0.0	$0.62^{+0.48}_{-0.38}$	$0.61^{+0.48}_{-0.37}$	$0.61^{+0.47}_{-0.37}$
d_L	2307	1831^{+373}_{-560}	1818^{+374}_{-556}	1859^{+378}_{-571}
$\phi_{\rm ref}$	0.0	$3.15^{+2.5}_{-2.52}$	$3.14^{+2.51}_{-2.5}$	$3.16^{+2.52}_{-2.52}$
$\rho^{\rm N}_{\rm mf}$	20.0	$19.07^{+0.09}_{-0.14}$	$19.05^{+0.09}_{-0.15}$	$19.02^{+0.17}_{-0.15}$
$e_{\rm gw}$	Injected	0.07	0.13	0.25
	Measured	$0.06^{+0.05}_{-0.05}$	$0.14^{+0.04}_{-0.04}$	$0.26^{+0.02}_{-0.03}$
$l_{\rm gw}$	Injected	1.96	0.81	4.27
	Measured	$2.25^{+1.19}_{-1.11}$	$1.33^{+1.7}_{-0.93}$	$4.32^{+0.63}_{-0.54}$

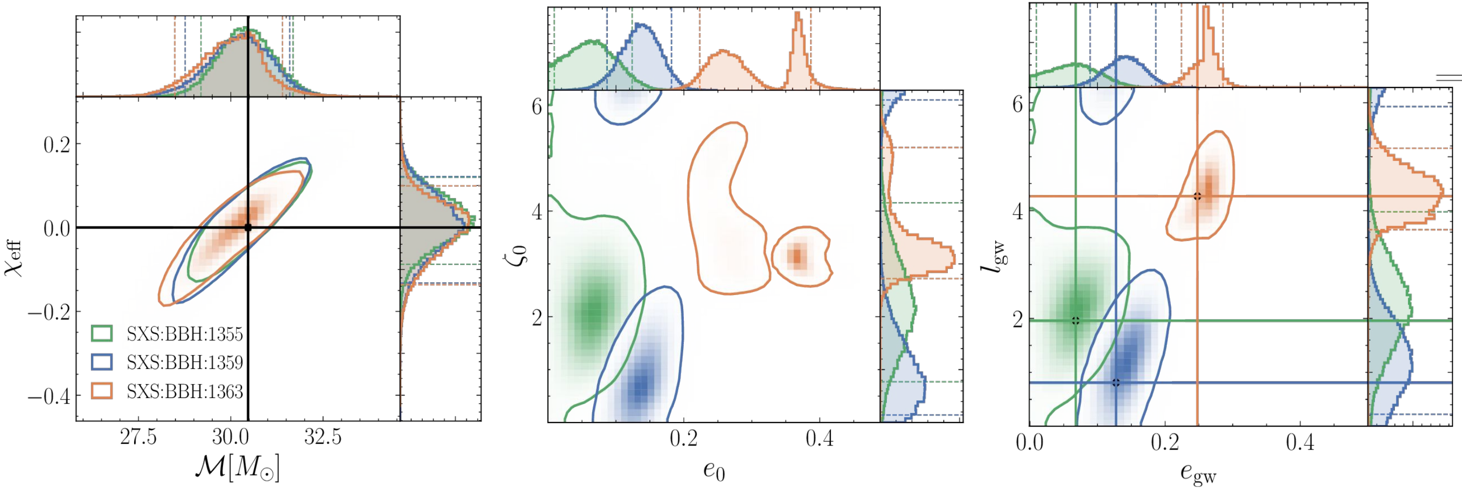

GW events: GW151226

- Analyze **GW151226** with **SEOBNRv4E_opt** (low total mass event).

  Comparison against **IMRPhenomXPHM** from GWTC-2.1.

- Differences between posteriors due to **spin-precession** and **distinct baselines of the approximants**.

Event	Waveform	$M/M_\odot$	$\mathcal{M}/M_\odot$	$1/q$	$\chi_{\rm eff}$	$e_{\rm gw}$	$l_{\rm gw}$	$\theta_{\rm JN}$	d_L	$\log\mathcal{BF}$
GW151226 ($f_{\rm start}=20$Hz)	SEOBNRv4E_opt	$22.61^{+1.97}_{-0.43}$	$9.66^{+0.05}_{-0.07}$	$0.7^{+0.23}_{-0.27}$	$0.15^{+0.09}_{-0.05}$	$0.05^{+0.05}_{-0.04}$	$3.02^{+2.57}_{-2.35}$	$1.93^{+0.87}_{-1.55}$	483^{+153}_{-170}	$33.2^{+0.1}_{-0.1}$
	IMRPhenomXPHM	$23.71^{+6.13}_{-1.36}$	$9.71^{+0.06}_{-0.05}$	$0.52^{+0.35}_{-0.29}$	$0.2^{+0.17}_{-0.07}$	-	-	$0.87^{+1.94}_{-0.57}$	471^{+124}_{-154}	$47.6^{+0.1}_{-0.1}$

- **No clear evidence of eccentricity**, consistent with [O'Shea+2021] using **TEOBResumS-Dali**.

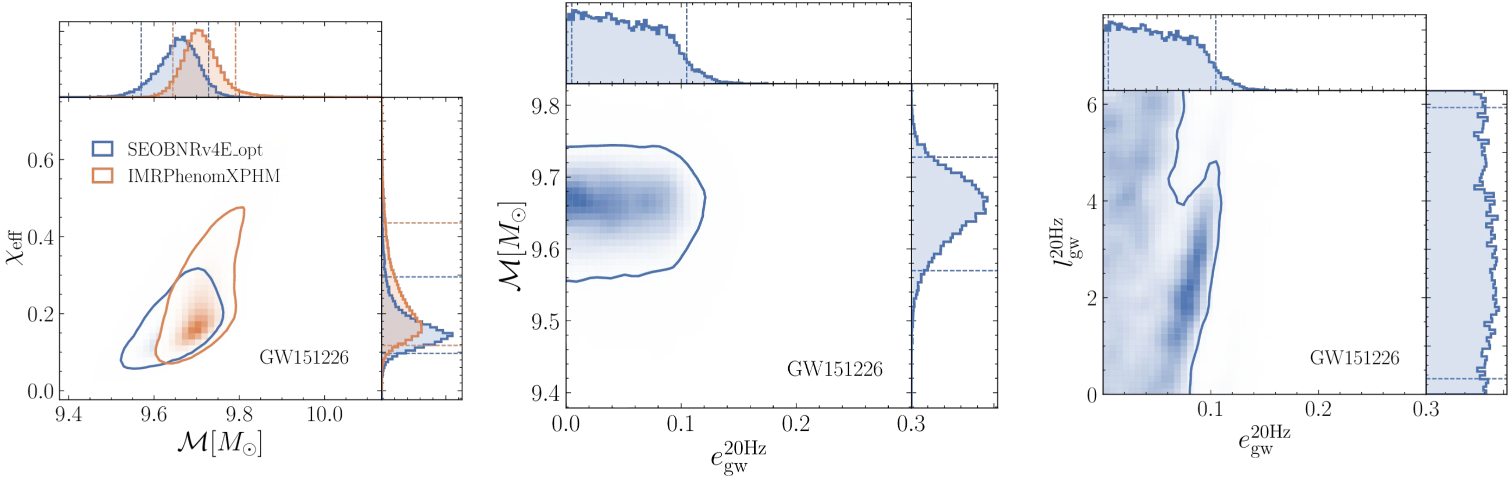

GW events: GW190521

- Analyze **GW190521** with **SEOBNRv4EHM_opt** (f_{min} =5.5Hz).
- Comparison against **SEOBNRv4PHM** from GWTC-2.1.
- Differences between posteriors due to **spin-precession**.
- **Uninformative GW mean anomaly and no clear measurement of GW eccentricity**.

Event	Waveform	$M/M_\odot$	$\mathcal{M}/M_\odot$	$1/q$	$\chi_{\rm eff}$	$e_{\rm gw}$	$l_{\rm gw}$	$\theta_{\rm JN}$	d_L	$\log \mathcal{BF}$
GW190521 ($f_{\rm start}$ = 5.5Hz)	SEOBNRv4E_opt	$259.92^{+21.63}_{-20.06}$	$111.15^{+9.88}_{-12.69}$	$0.74^{+0.2}_{-0.25}$	$0.02^{+0.23}_{-0.21}$	$0.15^{+0.12}_{-0.12}$	$3.14^{+2.26}_{-2.28}$	$1.27^{+1.43}_{-0.86}$	3924^{+1434}_{-1460}	$77.8^{+0.1}_{-0.1}$
	SEOBNRv4EHM_opt	$253.97^{+21.48}_{-24.94}$	$108.4^{+10.56}_{-15.27}$	$0.72^{+0.22}_{-0.24}$	$-0.01^{+0.21}_{-0.26}$	$0.15^{+0.12}_{-0.12}$	$3.16^{+2.25}_{-2.3}$	$0.88^{+1.89}_{-0.55}$	4172^{+1262}_{-1286}	$78.6^{+0.1}_{-0.1}$
	SEOBNRv4PHM	$279.54^{+36.74}_{-28.65}$	$118.13^{+12.94}_{-13.15}$	$0.74^{+0.2}_{-0.31}$	$0.06^{+0.26}_{-0.27}$	-	-	$1.39^{+1.28}_{-0.93}$	3964^{+1557}_{-1474}	-

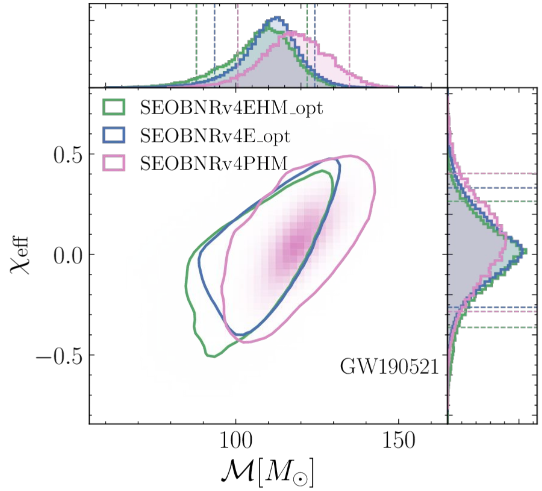

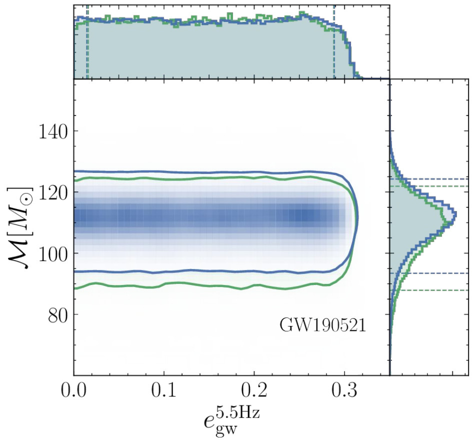

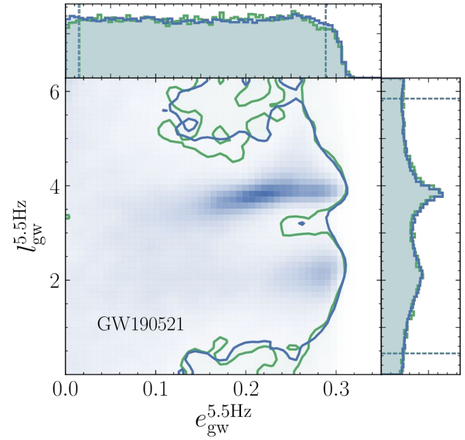

Conclusions

- We present new initial conditions at an **orbit-average frequency** for **SEOBNRv4EHM.**

- We introduce **SEOBNRv4EHM_opt** a **faster** version of SEOBNRv4EHM, which can be used for parameter estimation.

- We perform parameter estimation with **two eccentric parameters**, and show the biases of neglecting the radial phase parameter.

- **SEOBNRv4EHM_opt accurate against eccentric NR injections**. Use a waveform-based definition of eccentricity [Ramos-Buades+2022], and apply **gw_eccentricity**[Shaik+2023] package at post-processing (***pip install gw_eccentricity***).

- GW150914, GW151226 and GW190521 show **no clear evidence of eccentricity** with SEOBNRv4EHM_opt and uniform **$e_0 \epsilon [0,0.3]$ priors**.

Ongoing work:

- We are analyzing **all O3 events** in the GWTC-3 catalog using **DINGO** [Gupte+2023].

- New model **SEOBNRv5EHM ongoing** [Gamboa+2023], which will be deployed for **LVK review**.

Extra slides

Fast eccentric waveforms

- SEOBNRv4EHM relies on SEOBNRv4HM → **not computational efficient enough** for parameter estimation.

- Here, we present a faster version **SEOBNRv4EHM_opt**. Main modifications :
    - Usage of **optimized dynamics** and **Hamiltonian** from **SEOBNRv4_opt** [Devine+2016,Knowles+2018].
    - **Reduced** absolute and relative **ODE tolerances** from (10^{-9} ,10^{-10}) to (10^{-8}, 10^{-8}). Similarly to [O'Shea+2021] for TEOBResumS-Dali.

- **Assess accuracy** against SEOBNRv4EHM by computing the unfaithfulness for **4500 points** in the following parameter space:

$$q \in [1,50], \quad \chi_{1,2} \in [-0.9.0.9], \quad e_0 \in [0,0.5], \quad \zeta_0 \in [0.2\pi], \quad \iota = \pi/3 \quad \text{for} \quad M\omega_0 = 0.023$$

- Median mismatch over total mass range $M_T \in [20,300]M_\odot$ shows:
    - For **(2,|2|)-mode models** the median is **7.7 x 10^{-6}**.
    - For **higher-mode models** the median is **2.1 x 10^{-6}**.

- Overall **remarkable agreement** with **small tail** of large mismatches for corners of parameter spaces (**e_0>0.3 and high spins $\chi_{1,2}$>0.8**). Region out of the scope of this study.

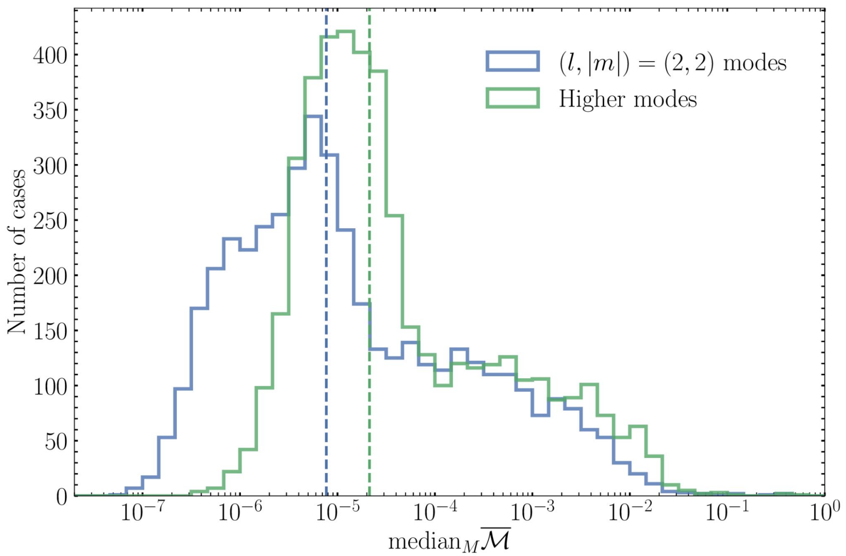

Fast eccentric waveforms

- Assess speed improvement of SEOBNRv4EHM_opt by **timing waveform evaluation** for two configurations:

$$q = 3, \quad \chi_1 = -0.5, \quad \chi_2 = 0.3, \quad \zeta_0 = 1, \quad M \in [20, 200]M_\odot, \quad e_0 = [0, 0.2] \quad \text{at} \quad f_{\text{start}} = 10\text{Hz}.$$

- Walltimes include all **modes l ≤ 4** and **sampling rate 8192 Hz**.

- Approximately **a factor 2-3 improvement in speed** for the configurations considered here.

- Sampling rate considered here quite high, typical PE applications use lower ones → **waveform evaluation times of O(100)ms**.

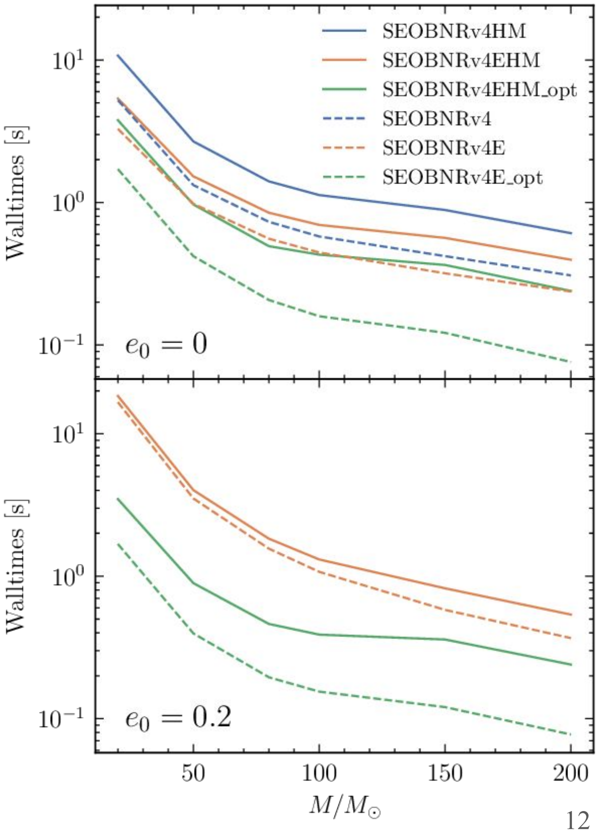

GW events: GW150914

- Analyze GW150914 with **SEOBNRv4EHM_opt** (l≤4 modes).
- Comparison against **SEOBNRv4PHM** from GWTC-2.1.
- Overall **good agreement with SEOBNRv4PHM**, and no clear measurement of eccentricity.

Event	Waveform	$M/M_\odot$	$\mathcal{M}/M_\odot$	$1/q$	$\chi_{\rm eff}$	$e_{\rm gw}$	$l_{\rm gw}$	$\theta_{\rm JN}$	d_L	$\log \mathcal{BF}$
GW150914 ($f_{\rm start}$ = 10Hz)	SEOBNRv4E_opt	$70.83^{+2.7}_{-2.88}$	$30.61^{+1.21}_{-1.32}$	$0.85^{+0.12}_{-0.16}$	$-0.04^{+0.08}_{-0.1}$	$0.08^{+0.1}_{-0.07}$	$3.31^{+2.2}_{-2.57}$	$2.48^{+0.4}_{-0.55}$	387^{+145}_{-133}	$283.9^{+0.1}_{-0.1}$
	SEOBNRv4EHM_opt	$70.89^{+2.42}_{-2.59}$	$30.72^{+1.08}_{-1.15}$	$0.89^{+0.09}_{-0.13}$	$-0.03^{+0.08}_{-0.09}$	$0.08^{+0.09}_{-0.06}$	$3.27^{+2.23}_{-2.49}$	$2.64^{+0.3}_{-0.37}$	440^{+117}_{-120}	$284.2^{+0.1}_{-0.1}$
	SEOBNRv4PHM	$71.32^{+3.39}_{-2.8}$	$30.92^{+1.51}_{-1.22}$	$0.9^{+0.08}_{-0.12}$	$-0.02^{+0.1}_{-0.09}$	-	-	$2.71^{+0.26}_{-0.59}$	492^{+103}_{-146}	-